Research Article

Journal of Environmental Nanotechnology

Studies on the Performance, Combustion, and Emissions of Hybrid Biofuel under Parametric Conditions

S. Ananthakumar[1*] and R. Barathiraja[2]

[1]Department of Mechanical Engineering, Government College of Engineering, Tirunelveli, TN, India
[2]Department of Mechanical Engineering, Mahakavi Bharathiyar College of Engineering and Technology, Tirunelveli, TN, India
Received: 26.01.2025 Accepted: 15.03.2025 Published: 30.03.2025
*ananth202004@gmail.com

ABSTRACT

The current study is aimed at the resolution of engine issues associated with higher viscosities found in biodiesel, such as rubber seed oil, through the blending of waste plastic oil. The experiments involved using a hybrid biodiesel made by blending rubber seed oil with waste plastic oil in volume proportions of 20%, 30%, and 40%. The results demonstrate that the hybrid alternative biodiesel, which comprises a blend of 20% rubber seed oil and 80% waste plastic oil (denoted as R 20 P 80), provides a brake thermal efficiency of 25.8% and a brake specific fuel consumption of 0.41 kg/kW-h. In addition, the R 20 P 80 blend exhibits higher oxides of nitrogen emissions by approximately 100 ppm and an increase of 0.07% volume in carbon monoxide emissions than that of diesel at maximum load. Additionally, the hydrocarbon releases are about 5 ppm higher, and the smoke opacity emission increases by 1% at full load for the R 20 P 80 blend compared to diesel. The findings imply that this hybrid biodiesel holds promise for use in a range of industries, including transportation, power generation, cultivation and farming, industrial and commercial applications, marine and shipping, aviation, residential heating, military applications, public transportation, off-road and recreational vehicles, and more.

Keywords: Combustion; Emission; Performance; Waste plastic oil; Rubber seed oil.

1. INTRODUCTION

Several research studies are focusing on lessening the paucity of petroleum and coal in the twenty-first century. Hence, it is necessary to identify readily available alternative fuels. Biodiesel is the best substitute for fossil fuels. In the present scenario, there are two methods available for operating a compression ignition (CI) engine with biodiesel; the first method is adapting a CI engine to biodiesel, and the second is adapting biodiesel to a CI engine. Given the scarcity of diesel and the availability of vegetable oil in agricultural countries like India, opting for the first method is a suitable choice. In a two-step transesterification procedure created by (Ramadhas *et al.* 2005a), high FFA (free fatty acid) oils are transformed into mono-esters, where crucial biodiesel characteristics, including cloud point, pour point, flash point, and specific gravity are determined and contrasted with that of diesel. Ikwuagwu *et al.* (2000) extracted *Hevea brasiliensis* seed oil, determined its physical and chemical characteristics, and found that monoesters were a more promising alternative to straight rubber seed oil (RSO) as a potential diesel fuel.

Miandad *et al.* (2017) examined the impact of different waste plastic types on pyrolysis oil. They found that polystyrene plastic waste resulted in the highest liquid oil production (80.8%) and contained 48.3% styrene. Ioannis *et al.* (2017) produced the pyrolysis oils from LDPE700 low density polyethylene and EVA900 ethylene-vinyl acetate at 700 °C and 900 °C, respectively. They found that the CI engine can run steadily on both pyrolysis oil blends. The LDPE700 polyethylene oil exhibited a performance almost similar to diesel, whereas the EVA900 had lower brake thermal efficiency, a longer ignition delay, higher oxides of nitrogen (NO_x) and unburned hydrocarbon (HC) emissions, and lower carbon monoxide (CO) emissions. Ramadhas *et al.* (2005b) created a two-step transesterification process that consists of an acid and an alkaline process to yield biodiesel from high free-fat acid plant oils. This biodiesel from RSO can be utilized in CI engines without alterations. It was also established that lesser blends increase brake thermal efficiency (BTHE), reduce brake specific fuel consumption (BSFC), and dissipate emanations. Reshad *et al.* (2015) utilized an ultrasonic horn and bath to improve the production of rubber seed oil methyl ester (RSOME). They did this by trans-esterifying esterified rubber seed oil. They found that at 80% load and with a 10% blend, the CI engine enhances BTHE and decreases NO_x and CO releases. The CI engine performance and emission using a blend of diesel and Jatropha biodiesel have been studied by Ambarish *et al.* (2014). It was observed that BSFC increases with a

greater proportion of biodiesel in the mixture. Also, they found that for the biodiesel blends, the CI engine can improve HC and CO and increase NO_x releases.

Pritinika and Muruga (2013) evaluated the emissions and performance factors of a diesel engine operated with used transformer oil (UTO) and six of its diesel mixtures. They found that UTO and its diesel blends have greater BTHE and decreased smoke than diesel and also have higher NOx emissions. Nantha and Thundil (2015) found that using different blends of *Pongamia* biodiesel in a CI engine led to a small drop in performance, but it also cut HC, CO, and smoke releases compared with diesel. In their study, Sureshkumar *et al.* (2008) discovered that engine performance and emissions are enhanced when using mixtures of up to 40% by volume of *Pongamia pinnata* methyl ester (PPME) with diesel. Also, they found that the use of PPME blends can help achieve rural economic development, environmental protection, and energy economy. According to Gumus and Kasifoglu, (2010) findings, apricot seed biodiesel and its mixtures can be utilised in CI engines without alteration. Lesser concentrations of the blend were observed to yield enhanced engine performance and reduced emissions. Ozcanli *et al.* (2012) assessed the emissions and performance of castor oil and its mixture with diesel, showing a reduction in CO and carbon dioxide (CO_2) releases compared to that of diesel but an increase in NO_x releases. Moreover, they found that the engine power decreased by a maximum of 4.12% with the B25 blend.

Nurun *et al.* (2009) studied cottonseed methyl ester production and its effects on emissions and engine performance. They also found that particulate emissions were reduced by 24% with 20% biodiesel mixtures, and smoke emissions were reduced by 14% with 10% biodiesel mixtures compared to diesel. According to Chauhan *et al.* (2012), Jatropha biodiesel and its mixtures can be utilized in a CI engine deprived of any modifications, demonstrating comparable performance and lower emissions. The result found that the ignition of biodiesel starts earlier than diesel fuel, and the peak cylinder pressure is lower for biodiesel. Atul and Avinash (2014) discovered that Karanja biodiesel blends can be directly employed in a transportation engine, up to a 20% blend, without requiring any modifications. Also, they found the maximum torque to be higher with 10% and 20% Karanja oil methyl ester (KOME) blends, lower emissions, and less smoke. The characteristics of a CI engine using rapeseed oil and its mixtures were investigated by Buyukkaya *et al.* (2010). The author found no changes in power output between B5 fuels and diesel, and low-concentration blends (B20 and lower) show potential for complete usage in the original CI engines.

Vijayaraj and Sathiyagnanam (2015) analyzed the features of a CI engine using mango seed oil and its mixture with diesel. They observed that the B25 blend exhibited enhanced engine characteristics. Muralidharan *et al.* (2011) examined the features of a variable compression ratio (VCR) engine operated with waste cooking oil and its mixtures. They noticed that the BTHE of biodiesel mixtures is greater than diesel and also observed that there is a reduction in BSFC with an increase in load. Subbarayan and Senthil (2015) investigated the features of a diesel engine operated with pumpkin seed oil, cottonseed oil methyl ester (COME), and their mixtures with diesel using exhaust gas recirculation (EGR). They found that COME-EGR gave lesser emissions compared to conventional methods; also, B25 -COME with EGR gave the minimum releases and improved performance, and there is a decrease in NO_x release with EGR. Sahoo and Das, (2009a) examined the burning of Karanja, Jatropha, and Polanga methyl ester in a CI engine and found that Polanga biodiesel had the highest peak cylinder pressure. They also found that the ignition delays were smaller for pure Jatropha, Polanga methyl ester, and Karanja than diesel.

Sahoo *et al.* (2009b) assessed the features of Karanja, Jatropha, and Polanga methyl ester mixtures (B20 and B50) in a tractor engine. The authors found a decrease in particulate matter (PM) and HC and a slight rise in CO and NOx for all the biodiesel blends. The engine operated on sesame oil methyl ester showed higher BTHE and lesser releases compared to Honge and Jatropha biodiesel, according to Banapurmath *et al.* (2008). Rakopoulos *et al.* (2006) found that vegetable oil and bio-diesel mixtures can be securely and profitably used in a CI engine, with similar performance to neat diesel. Saravanan *et al.* (2009) examined the possibility of utilizing a crude rice bran methyl ester (CRBME) blend as a tested fuel for locomotive and stationary CI engines and found it to have better emission characteristics than diesel. The authors found that the CRBME blend showed significant reductions in HC, CO, and particulates and a marginal rise in NO_x releases compared to diesel. Chakrabarti *et al.* (2013) evaluated that Pongame B20 fuel had better environmental emissions and engine features compared to Jatropha B20 (20 % biodiesel and 80 % diesel) fuel in Pakistan.

Ananthakumar *et al.* (2017) studied the important characteristics of VCR engines operated with waste plastic oil (WPO) and its mixtures with diethyl ether (DEE) additive. The results indicated that BTHE increases for all the mixtures when the compression ratio (CR) increases from 12:1 to 20:1. The BSFC of the WPO and its mixtures was higher compared to that of diesel. According to Mani *et al.* (2009), the WPO was used as fuel in a CI engine, and though CO and HC exhalations were relatively excessive, the BTHE of the WPO was equal to that of diesel. Senthilkumar and Sankaranarayanan (2016) investigated the diesel engine characteristics at WPO. The findings demonstrate that WPO increases carbon monoxide, NOx, and HC

pollution more rapidly than diesel. By using WPO mixes in a CI engine, Kumar *et al.* (2013) analyzed the performance and emission characteristics; they found that WPO mixes have a lower BTHE and a higher BSFC and exhaust gas temperature.

Overall, the literature suggests that biodiesel remains a promising and environment-friendly substitute for conventional diesel. However, to fully realize its potential, further research and development are needed to address technical challenges, improve engine performance, and enhance the sustainability of feedstock sourcing and production processes. No prior research has been undertaken on the utilization of a particular hybrid alternative biodiesel, which consists of blends of rubber seed oil and waste plastic oil. To fill this research gap, a novel experimental investigation was conducted using different blends, namely R 20 P 80, R 30 P 70, and R 40 P 60. The primary objective of this work is to compare and analyze how various hybrid biodiesel blends, such as R 20 P 80, R 30 P 70, and R 40 P 60, affect the combustion, emissions, and performance of CI engines. Subsequently, these findings were compared with those obtained from diesel and pure waste plastic oil. This analysis is valuable for engine manufacturers to use biodiesel because of their commitment to sustainability, meeting regulatory requirements, catering to market demand, exploring new technologies, and enhancing energy security. By embracing biodiesel as a viable fuel option, engine manufacturers can contribute to a greener and more sustainable future for the transportation industry.

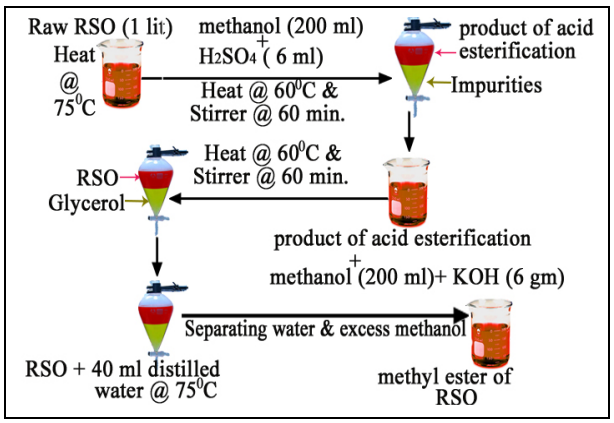


Fig. 1: Schematic diagram of RSO esterification process

2. MATERIALS AND METHODS

2.1 Production of Methyl Ester of Rubber Seed Oil

In Fig. 1, a schematic diagram of the RSO esterification process is presented. The process takes place in a 1000 ml round bottom flask and a 1250 ml separating funnel equipped with a control valve to prevent oil leakage. Initially, 1000 ml of crude RSO is warmed up to 75 °C to eliminate moisture content. Then, 200 ml of CH_3OH (methanol) and 6 ml of sulfuric acid (H_2SO_4) are added to the preheated RSO. The resultant mixture is stimulated using a magnetic agitator at 1000 rpm, and the temperature is maintained at 60 °C for 60 minutes. After stirring, the oil is shifted to the splitting funnel, where surplus methanol and the catalyst settle as impurities in the bottom layer, while the pre-treated rubber seed oil settles in the top layer after 12 to 14 hours. This pre-treated oil is collected for the alkaline esterification process. The acid esterification process reduces the FFA content in the raw RSO from 22% to a lesser amount of 2%.

During alkaline esterification, 1000 ml of pre-treated oil is combined with 200 ml of CH_3OH and 6 g of KOH catalyst in the flask. The mixture is stirred using a magnetic stirrer at 1000 rpm, at 60 °C for 60 minutes. After heating, the pre-treated oil is shifted to the splitting funnel. The partition occurs after 10 to 12 hours. The top layer contains the methyl ester of RSO, while the bottom layer comprises catalysts, glycerine, unused methanol, and other impurities. The collected methyl ester is then thoroughly cleansed with 40 ml of warm distilled water at 75 °C to remove any excess methanol. The settled water and excess impurities are removed from the bottom of the separating funnel.

2.2 Production of the Waste Plastic Oil

Fig. 2 illustrates the schematic diagram of the pyrolysis plant, which comprises a reactor and condenser unit. The reactor, made of stainless steel and measuring 1300 mm in diameter, is enclosed by a thin sheet. To facilitate the pyrolysis process, three 1500 W electrical heater coils are affixed to the reactor. Glass wool is used as an insulator, positioned between the reactor and the thin sheet. The reactor is equipped with a mechanical stirrer, operated by a motor, along with a safety valve, a pressure gauge, a feed hopper with a control valve, a K-type thermocouple, a hand hole, and a control panel. The mechanical stirrer is used to thoroughly mix the mixture and maintain a controlled temperature ranging from 500 to 700 °C inside the reactor. In the event of excess pressure build-up, the safety valve is responsible for releasing it. The temperature inside the reactor is monitored and measured by the thermocouple, and this information is displayed on the control panel indicator, managed by the controller.

Upon completion of the pyrolysis process, about 20 to 25% of the waste material is removed through a hand hole with a stop cock located at the bottom of the reactor. The outlet of the reactor is connected to a condenser, which comprises a water container and a cooling coil. The cooling coil is constructed from a stainless-steel duct of 1800 mm length and 20 mm diameter. It is placed inside a water container with a height of 500 mm and a diameter of 300 mm. The

container is equipped with inlet and outlet valves to circulate water. The plastic vapours are condensed in the cooling coil, and the resulting liquid is collected in a fuel collection tank made of stainless steel. The delivery time for the liquid fuel is approximately 3.5 hours from the start of the pyrolysis process. The uncondensed gas is directed through an AVL 444 DiGas Analyzer and then passed through a flame arrester containing water to prevent backfire. Subsequently, the washed, uncondensed gas flows through a burner to achieve a blue flame, which helps reduce pollutants in the atmosphere.

2.3 Preparation of RSO-WPO Blends

The process of mixing a high-viscosity fuel with a low-viscosity fuel is commonly referred to as blending. In this study, rubber seed oil is blended with waste plastic oil in various volume-based proportions, ranging from 20% to 40% in regular increments of 10%. These blends are denoted as R 20 P 80, R 30 P 70, and R 40 P 60. To achieve a homogeneous solution, the blends are thoroughly stirred using a magnetic stirrer. Fig. 3 displays the photographic images of RSO, WPO, and their blends.

Table 1 shows how different blends of RSO and WPO measure up in terms of their physical and chemical features, such as net calorific value, flash point, specific gravity, and kinematic viscosity.



Fig. 3: RSO, WPO, and their blends

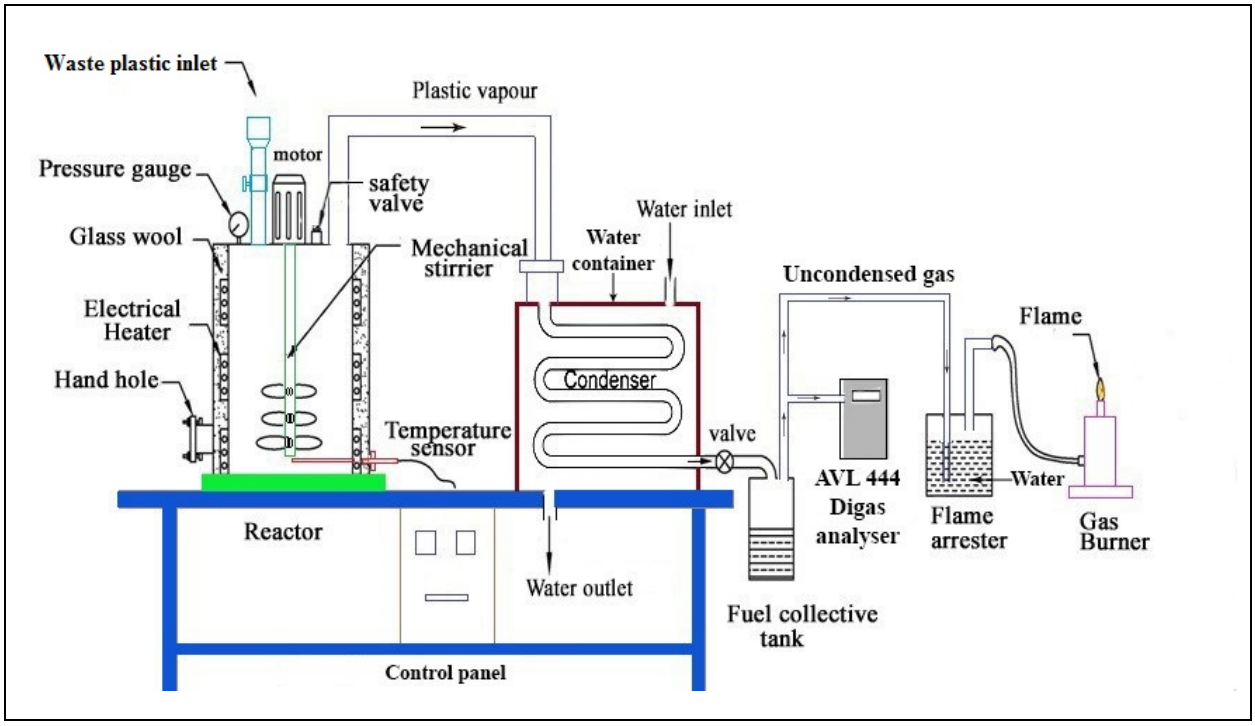


Fig. 2: Schematic diagram of the Pyrolysis plant

3. EXPERIMENTAL SETUP

Fig. 4 displays a photographic image of the experimental setup. For this study, a Kirloskar (AV1)-based vertical, direct-injection, water-cooled engine with a calculated power of 3.7 kW at 1500 rpm is employed. The comprehensive specifications of the test engine are presented in Table 2.

4. RESULTS AND DISCUSSION

The experimental investigations are conducted using a single-cylinder, four-stroke, and water-cooled DI engine. The engine is operated on different blends of RSO-WPO, diesel, and neat WPO, all at a compression ratio of 16:1. The blends consist of varying RSO percentages, ranging from 20% to 40% in regular 10%

intervals, based on volume. By comparing the emission, combustion, and performance characteristics of these different mixtures, an optimum blend is selected for further investigation.

4.1 Pressure-Crank Angle Diagram

The pressure variation in the cylinder concerning the crank angle plays a crucial part in the fuel's performance analysis. In CI engines, the cylinder's peak pressure is influenced by the initial stages of the combustion rate. The combustion rate is affected by factors such as the type of fuel used in uncontrolled or premixed combustion, the duration of the ignition delay, mixture preparation throughout the delay period, and the spray envelope. Fig. 5 depicts the pressure-crank angle diagram under full load conditions for the fuels that were tested. The observation reveals that, under full load, the maximum cylinder pressure is greater for the three blends and WPO in comparison to diesel. The combustion of the three blends commences later, leading to a slight increase in peak pressure in comparison to diesel. For diesel fuel, the cylinder experiences a peak pressure of approximately 62 bar, while for waste plastic oil, it reaches around 67 bar. For the R 20 P 80, R 30 P 70, and R 40 P 60 blends, their respective cylinder peak pressures are 66, 65, and 63 bar, respectively. Notably, the maximum cylinder pressure for WPO exceeds that of diesel and the three mixtures, owing to its shorter ignition delay. The blends also exhibit greater maximum cylinder pressure under full load than diesel fuel, possibly owing to their elevated oxygen content and specific fuel consumption.

Table 1. Physiochemical properties of RSO and WPO blends

Properties	Diesel	RSOME	WPO	R 20 P 80	R 30 P 70	R 40 P 60
Specific gravity at 15 °C	0.82	0.8102	0.9155	0.893	0.882	0.871
Net calorific value, kJ/kg	44800	38650	43340	41362.4	40605.1	39847.8
Flash point, °C	50	66	54	56	58	59
Fire point, °C	57	68	56	58	60	61
Kinematic viscosity at 40 °C, cSt	2	12.75	3.18	3.704	3.966	4.228
Cetane index	50	56	51	38.4	40.6	43
Water content, wt. %	0.025	0.3	0.01	0.065	0.094	0.124
Oxygen by difference, %	Nil	22	1.5	5.6	7.65	9.7

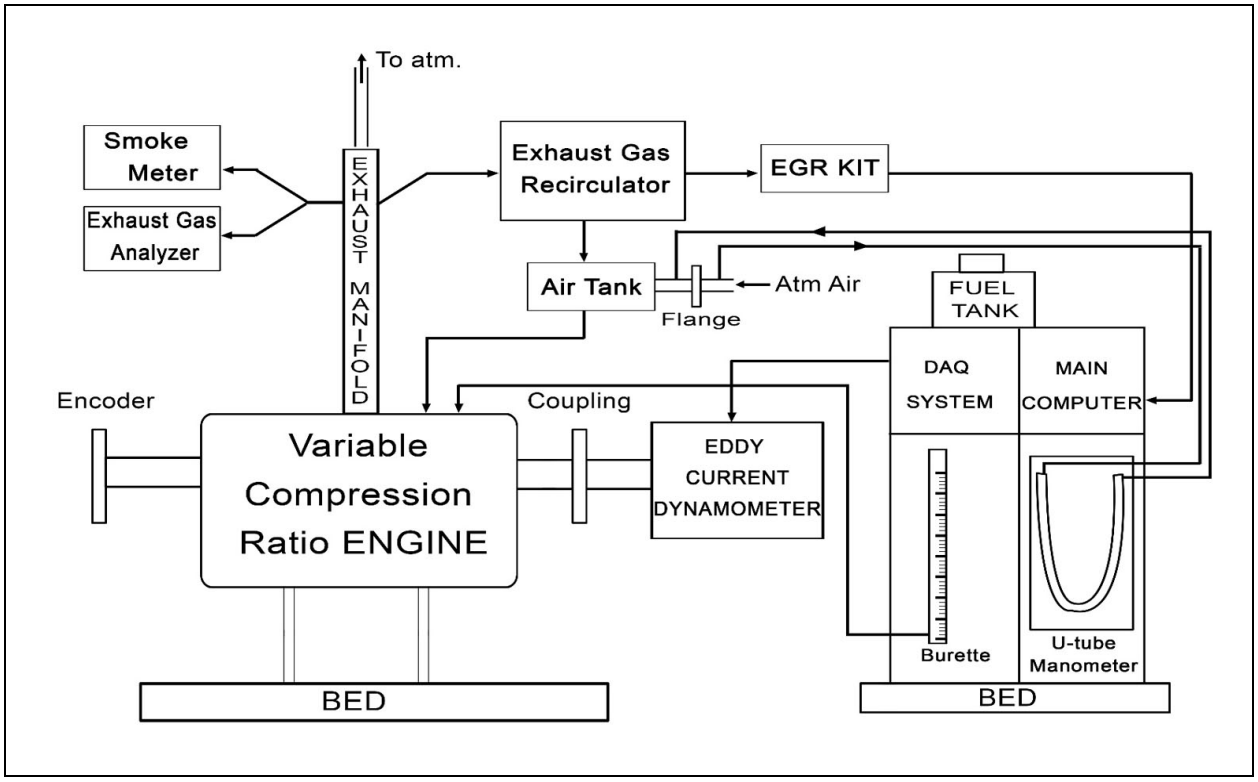


Fig. 4: Experimental setup

Table 2. Technical specifications of the Experimental setup

Particulars	Specifications
Make and Model	Variable compression ratio, multi-fuel, vertical, water-cooled, direct injection, naturally aspirated engine. Engine modification for changing the compression ratio arrangement is made by Legion Brothers, Bangalore. The base crankcase is made by the Kirloskar AV1 engine.
Compression ratio range	6:1 to 20:1
Rated brake power	3.7 kW
Rated speed	1500 rpm
No. of cylinders / No. of strokes	01 / 04
Bore x Stroke	80 x 110 mm
Displacement volume	552.64 cc
Nozzle opening pressure	200 bar
Make of the fuel injector	Bosch - DLLA 110S 1030E
Diameter and Number of nozzle holes	3 ± 0.2 mm and 3 holes
Maximum load	10 kg
Software	"Engine Test Express v14" Engine performance analysis software

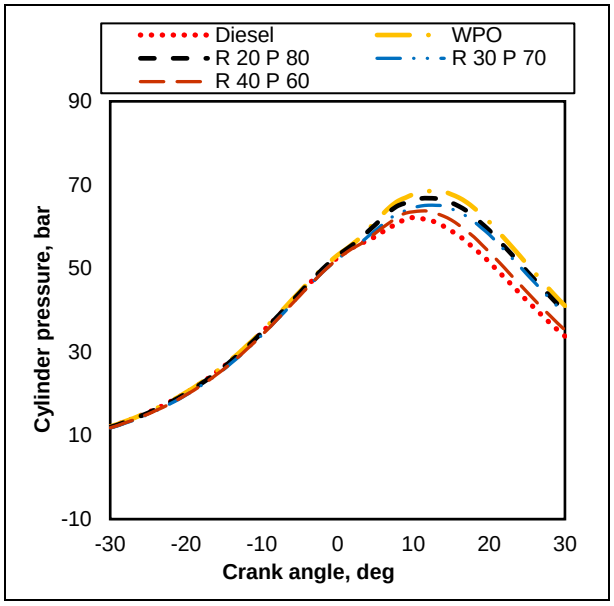


Fig. 5: Pressure-Crank angle diagram at full load

4.2 Ignition Delay

Ignition delay refers to the time interval between the initiation of injection and the commencement of fuel combustion, quantified in degrees of crank angle within a diesel engine. It is a critical parameter that helps determine the cylinder's maximum pressure, heat release rate, and pressure rise. It is influenced by various factors, including the type of fuel, fuel quality, atomization, engine speed, air-fuel ratio, intake air pressure, and temperature. The delay period is measured from the moment where the rate of the heat release curve initiates an ascent from zero. The density and viscosity of the three blends exhibit a slight increase compared to those of diesel. Consequently, the identical injection timing of 23 °bTDC (before top dead center) was adopted for all the tested fuels. Fig. 6 depicts the changes in ignition delay at varying loads for all the fuels that were tested. Observations reveal a reduction in ignition delay with an increase in load. This decrease can be attributed to the elevated temperature of the combustion chamber walls during injection and a decrease in exhaust gas dilution under heavier load conditions.

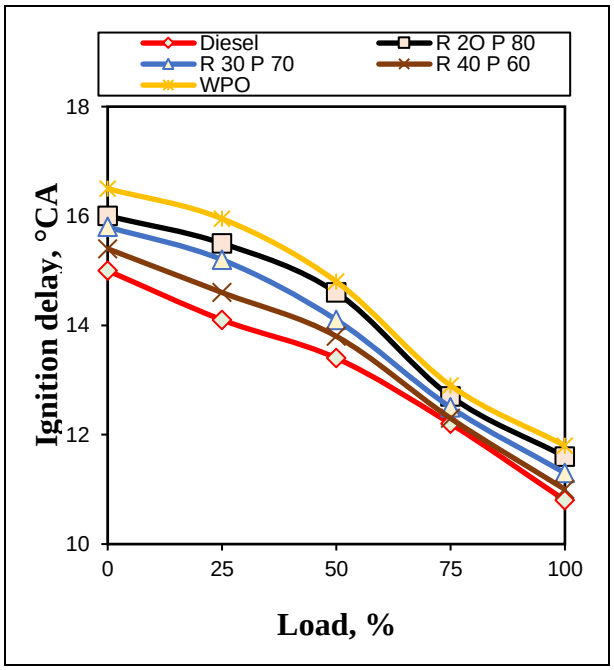


Fig. 6: Variation of Ignition delay with Load

The decrease in ignition delay for all three blends is linked to their attributes of increased surface area-to-volume ratio, rapid evaporation rate, and enhanced ignition properties. The shorter ignition delay for the three blends, compared to WPO, can be attributed to chemical reactions occurring during injection at high temperatures. These reactions lead to the degradation of higher-molecular-weight components into lower-molecular-weight constituents. For diesel, the ignition delay varies from 15 °CA (crank angle) under zero load to 10.8 °CA at 100% load; for the R 20 P 80 blend, it fluctuates from 16 °CA under zero load to 11.6 °CA at 100% load. Similarly, for the R 30 P 70 blend, it differs from 15.8 °CA under zero load to 11.3 °CA at full load, whereas in the R 40 P 60 blend, it differs from 15.4 °CA under zero load to 11 °CA at full load. For the neat WPO, the ignition delay fluctuates from 16.5 °CA under zero load to 11.8 °CA at 100% load. The longer ignition delay period of neat WPO in comparison to diesel results from its elevated viscosity, lesser cetane number, and greater heat release rate. These factors contribute to an increase in maximum cylinder pressure. The ignition delay is approximately 2.2 °CA longer at no load and 1.5 °CA longer under full load for pure waste plastic oil in comparison to diesel. The ignition delay decreases as the blend concentration increases. This is due to the higher oxygen levels in the blends.

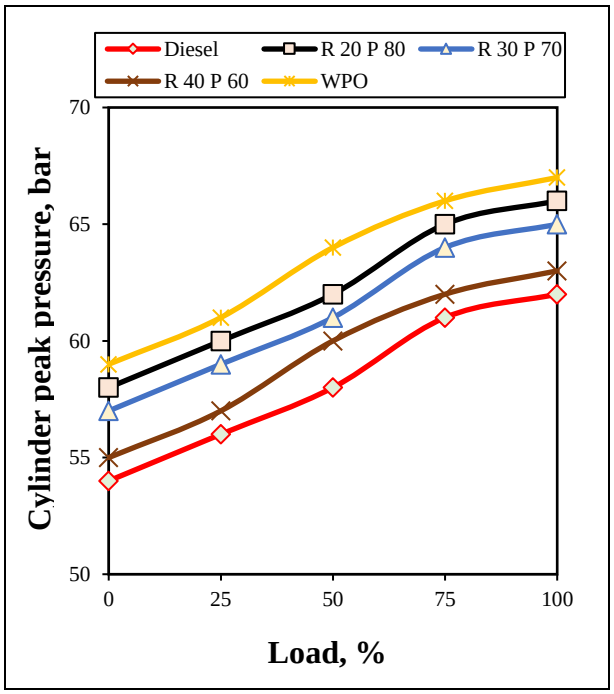


Fig. 7: Variation of Cylinder peak pressure with Load

4.3 Cylinder Peak Pressure

Fig. 7 displays the changes in cylinder peak pressure with varying load conditions for all the fuels examined in this study. The cylinder peak pressure in a CI engine primarily relies on the quantity of fuel involved in the uncontrolled combustion phase, the fuel accumulation during the delay period, and the combustion pace during the early phases of premixed combustion. With an escalation in load, there is a corresponding augmentation in peak cylinder pressure. Notably, the peak cylinder pressure for both neat WPO and RSO-WPO blends surpasses that of diesel. The peak cylinder pressure for diesel varies from 54 bar under zero load to 62 bar at 100% load, and for WPO blend, it increases from 59 bar under zero load to 67 bar at 100% load. For R 20 P 80 blend, it rises from 58 bar under zero load to 66 bar at 100% load; for R 30 P 70 blend, it increases from 57 bar under zero load to 65 bar at 100% load; and for R 40 P 60 blend, it increases from 55 bar under zero load to 63 bar at 100% load. Comparatively, the peak cylinder pressures for RSO-WPO mixtures are lower than those of WPO. This lower peak pressure in blends may be attributed to slow vaporization and combustion owing to the higher viscosity of RSO. However, the three mixtures produce comparable peak pressure with neat WPO owing to an enhancement in the air-fuel mixture preparation. The higher heat release and ignition delay during the premixed combustion stage are the reasons for the greater peak pressure in the cylinder for RSO-WPO blends as opposed to diesel. Additionally, the inclusion of 22% oxygen in RSO enhances combustion, leading to higher cylinder peak pressure.

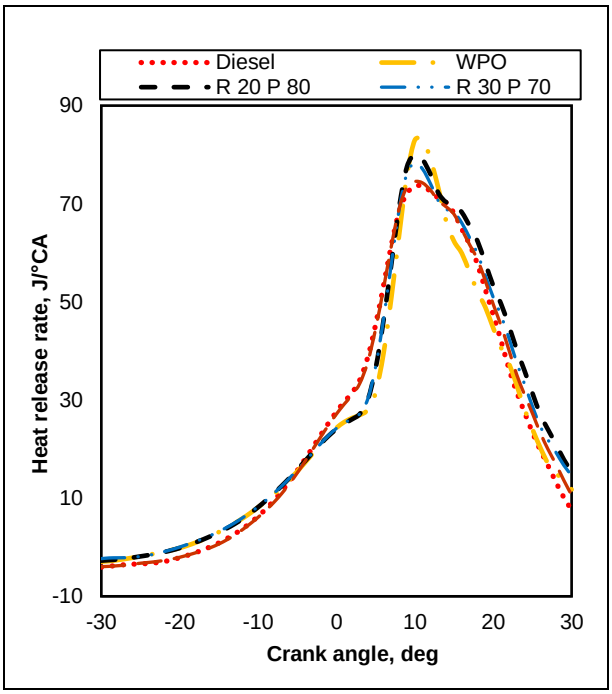


Fig. 8 Variation of HRR with Crank angle at full load

4.4 Heat Release Rate

A comprehensive understanding of the heat release rate (HRR) resulting from combustion is crucial for analyzing engine performance characteristics, NO_x emissions, and the cooling system requirements of an

engine. The HRR also governs the level of pressure exerted on the cylinder and the exhaust releases in an engine. The combustion procedure within a diesel engine is characterized by three stages: air-fuel mixing, controlled or diffusion combustion, and uncontrolled or premixed combustion. The uncontrolled or premixed combustion phase extends from ignition initiation until the onset of the HRR curve. The controlled or diffusion combustion phase commences following the conclusion of the initial phase and endures until the culmination of the combustion process. The maximum HRR in the premixed combustion stage is predominantly influenced by the delay period, mixture composition, and combustion ratio. The HRR might attain a secondary peak or might not reach one at all. In the present investigation, the second peak does not seem to be significant during the diffusion combustion stage. Fig. 8 illustrates the variation in the rate of heat release at full load.

At full load, the blends and WPO exhibit a maximum HRR than those of diesel, primarily because of the bulk modulus characteristic of WPO. Diesel shows a maximum HRR of 73 J/°CA, while WPO exhibits 83 J/°CA owing to its extended ignition delay period. For the blends, the maximum HRR is 80 J/°CA for R 20 P 80, 78 J/°CA for R 30 P 70, and 74 J/°CA for R 40 P 60. During the diffusion combustion stage, the rate of combustion is regulated by the presence of the air-fuel mixture. The blends display a higher HRR than that of diesel due to their swifter combustion traits, the presence of oxygen in RSO, and the blends' rapid evaporation tendencies. However, the premixed combustion phase is closer to that of WPO, especially for lower blends like R 20 P 80 and R 30 P 70, owing to the lower viscosity of these blends.

4.5 Brake Thermal Efficiency

The BTHE denotes the proportion of brake power generated per cycle of an internal combustion engine in relation to the heat energy introduced through the fuel. This efficiency reflects how effectively the thermal energy from the fuel is transformed into mechanical energy within the engine. Fig. 9 illustrates the fluctuation of BTHE with different loads for various fuel mixtures, including diesel and neat WPO. As the engine load increases, its efficiency improves owing to the elevated in-cylinder temperature. At 100% load, the BTHE of diesel is 26.8%. For the engine running on various tested fuels, the BTHEs under 100% load are as follows: R 20 P 80 - 25.8%, R 30 P 70 - 25.2%, R 40 P 80 - 24.9%, and WPO - 23.4%. The brake thermal efficiencies of lower blends (R 20 P 80 and R 30 P 70) are closer to those of diesel due to their similar combustion behaviour, additional available oxygen molecules, lower blend viscosity, and lower rubber seed oil concentration. In contrast, the brake thermal efficiencies of the R 40 P 60 blend and waste plastic oil are significantly lower than that of diesel fuel because of the lower volatility and higher viscosity of rubber seed oil. These properties lead to poor formation and combustion of the air-fuel mixture, leading to reduced BTHE at higher mixtures. It is also noted that the reductions in BTHE occur with increasing rubber seed oil concentrations in the mixture. This decrement is attributed to the initiation of heat release closer to TDC for WPO, leading to a higher HRR than diesel. Consequently, a significant amount of heat is lost through the exhaust gases, contributing to a decrease in BTHE.

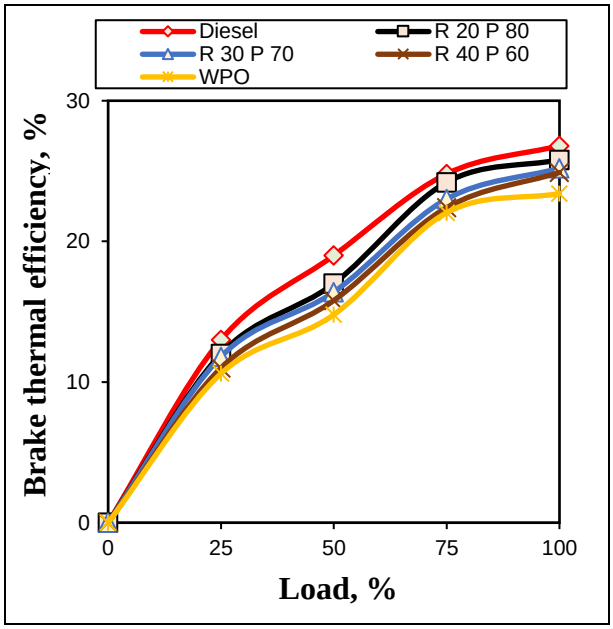


Fig. 9: Variation of BTE with Load

4.6 Brake Specific Fuel Consumption

The BSFC serves as a measure of engine efficiency, representing the relationship between the mass of fuel consumed and the engine's effective brake power output. Fig. 10 illustrates the deviation of BSFC with various loads for waste plastic oil, its RSO mixtures, and diesel. Observations reveal that as loads increase, BSFC reductions occur consistently across all tested fuels. At full load, BSFC values are 0.375 kg/kW-h for diesel and 0.465 kg/kW-h for WPO. For the R 20 P 80 blend, the BSFC is slightly higher compared to diesel because of its elevated density, viscosity, and lesser calorific value. However, throughout engine operation, the R 20 P 80 blend demonstrates the lowest BSFC among the three blends. This is attributed to its higher heating value, lower density, and viscosity, resulting in more efficient and complete combustion. On the other hand, the R 30 P 70, R 40 P 60 blends, and WPO exhibit higher BSFC than that of the R 20 P 80 blend. This could be due to the poorer fuel spray formed by R 30 P 70, R 40 P 60 blends, and WPO as an outcome of their elevated viscosity. Consequently, more fuel may be essential to develop the same power as diesel and the R 20 P 80 blend, especially when the fuel's calorific value is low.

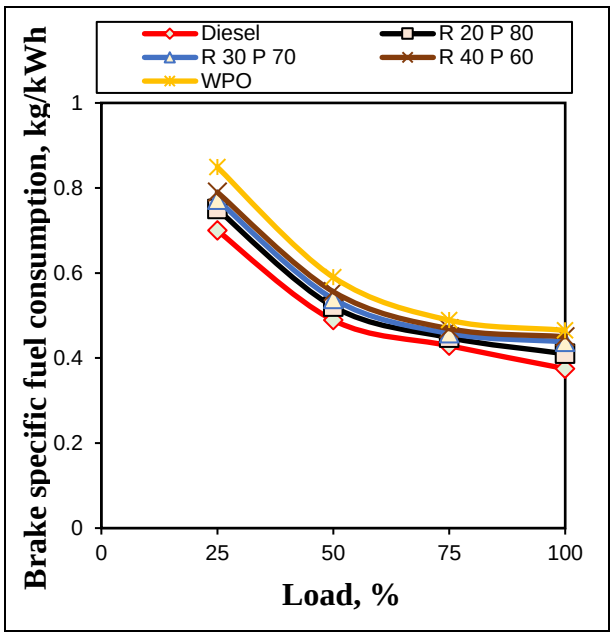


Fig. 10: Variation of BSFC with Load

4.7 Exhaust Gas Temperature

The exhaust gas temperature (EGT) represents the quantity of heat carried through the exhaust manifold by the exhaust gases. A lower EGT indicates high-quality combustion of the tested fuel within the combustion compartment and signifies the efficient utilization of the heat energy present in the fuel within an engine. Higher heating value, oxygen content, cetane number, density, and kinematic viscosity are the five most important physical and chemical properties that affect EGT. Fig. 11 illustrates the fluctuation of EGT with load. From the figure, it is to be noted that the EGT increases with load for both WPO and its RSO blends, in addition to diesel, since more fuel is burned to meet the power necessity. Specifically, the EGT rises from 230 °C at zero load to 455 °C at 100% load for WPO. Likewise, for diesel, it increases from 213 °C at zero load to 400 °C at 100% load.

At full load, the EGT for R 20 P 80, R 30 P 70, and R 40 P 60 blends increase to 410, 422, and 434 °C, respectively. In comparison to diesel, the EGT for WPO is higher by approximately 17°C at zero load and 55°C at 100% load because of its elevated rate of heat release. The presence of 1.5% oxygen in WPO contributes to improved combustion. The higher EGT in WPO, when compared to other tested fuels, can be attributed to the well-formed mixture and constructive combustion. The improved spread of combustion occurs due to an extended ignition delay throughout the combustion process. Moreover, the EGT increases with a rise in the concentration of rubber seed oil in the WPO mixture. This rise is primarily attributed to the higher boiling points of RSO constituents in comparison to WPO. Mixtures that do not undergo sufficient evaporation during the primary combustion phase and persist in burning during the later combustion phase lead to a minor elevation in EGT and a reduction in BTHE.

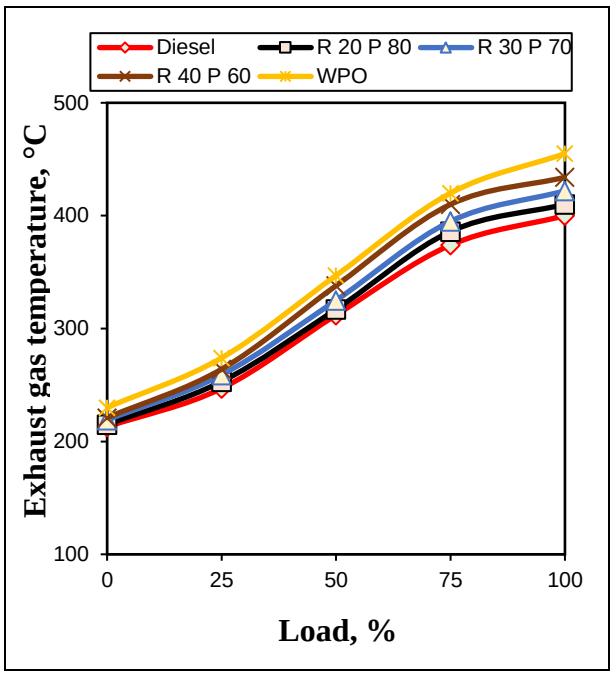


Fig. 11: Variation of EGT with Load

4.8 Oxides of Nitrogen Emissions

The emissions known as nitrogen oxides (NO_x) comprise nitric oxide (NO) and nitrogen dioxide (NO_2), frequently combined. NO_x releases are a combustion product comprising 10% to 30% NO_2, with the remainder being NO. Nitric oxide plays an important part in the oxides of nitrogen and is generated within the engine cylinder. These emissions result from oxidation occurring within the engine cylinder at 2200 K temperature. Breaking the triple bond of nitrogen requires substantial energy. Therefore, when the elevated combustion temperature aids in oxidation, NO_x emissions are generated. The formation of NO_x emissions is influenced by the oxygen concentration and temperature of cylinder combustion. Engines utilizing compression ignition usually function with air-fuel mixtures that lean towards excess air, resulting in elevated NO_x emissions.

NO_x releases from waste plastic oil and its RSO mixtures increase with a rise in loads. The presence of oxygen in RSO mixtures aids in improved combustion and a higher heat release rate, but it correspondingly leads to increased NO_x emissions. WPO contains approximately 1.5% oxygen. Fig. 12 illustrates the variation of NO_x emissions with different loads; as depicted, it is clear that the NO_x released from waste plastic oil is elevated throughout the entire load variation compared to those of diesel and RSO-WPO blends. In diesel engines, higher loads result in higher in-cylinder

temperatures due to the injection of a larger fuel amount, but the oxygen availability for NO_x formation is reduced because more oxygen is consumed for combustion, and the oxygen supply remains constant at all loads. The NO_x emissions' concentration increases from 160 ppm under zero load to 820 ppm at 100% load for diesel and from 287 ppm under zero load to 1010 ppm at 100% load for waste plastic oil. For the R 20 P 80 blend, it fluctuates from 205 ppm at zero load to 920 ppm at 100% load. Likewise, NO_x emission diverges from 196 ppm during zero load to 874 ppm at 100% load for the R 30 P 70 blend, and it fluctuates from 185 ppm during zero load to 833 ppm at full load for the R 40 P 60 blend.

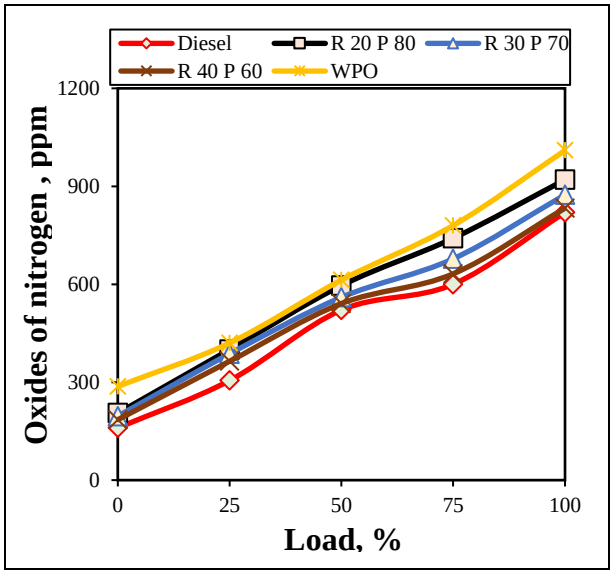


Fig. 12: Variation of Oxides of Nitrogen with Load

The higher NO_x emissions observed in waste plastic oil are attributed to its elevated aromatic content featuring a ring structure. This structural characteristic results in a higher rate of heat release and subsequently increases the cylinder temperature. In Fig. 12, the NO_x releases are lower for the three mixtures than for neat waste plastic oil. NO_x releases decrease with a rise in the proportion of rubber seed oil in the mixture. This reduction can be attributed to the higher viscosity of rubber seed oil, its lower volatility, lower heating value, and slower pre-mixed burning rate when compared to waste plastic oil.

4.9 Hydrocarbon Emissions

Hydrocarbon (HC) emissions serve as a valuable indicator of combustion inefficiency because they comprise unburned fuel. Typically, CI engines have a high capability to convert the air-fuel mixture into combustion products, achieving around 98% efficiency. As a result, HC emissions are generally lower since these engines consistently operate with lean fuel-air equivalence ratios overall. The primary factors contributing to the formation of HC emissions are the amount of hydrocarbon gases present in crevice areas and a comparatively stagnant lower temperature boundary layer beside the cylinder wall. This occurs because the flame does not propagate into these regions during combustion. Fig. 13 depicts the disparity of hydrocarbon emissions with different loads for the operated fuels. It is evident that for waste plastic oil, the hydrocarbon emission fluctuates between 45 ppm at zero load and 101 ppm at 100% load. Similarly, for the R 40 P 60 blend, HC fluctuates from 44 ppm at zero load to 98 ppm at 100% load. For the R 30 P 70 mixture, HC emission contrasts from 41 ppm at zero load to 93 ppm at 100% load, and for the R 20 P 80 blend, HC diverges from 39 ppm at zero load to 89 ppm at 100% load. In diesel, the hydrocarbon emission fluctuates between 35 ppm at zero load and 84 ppm at full load. HC emissions for WPO and its RSO mixtures are higher than diesel. Additionally, it can be noted that the HC emission increases with a rise in the proportion of rubber seed oil in the mixture, as well as with the load. The higher viscosity of RSO leads to larger fuel spray droplet sizes for its waste plastic oil blends compared to diesel. When these fuel blends are injected into the cylinder, they mix with air to form non-homogeneous rich and lean zones in the combustion compartment. Some fuel droplets in the rich regions do not fully respond due to a deficiency of oxygen, leading to incomplete incineration. This partial combustion is also responsible for the higher HC emissions in RSO-WPO blends compared to diesel.

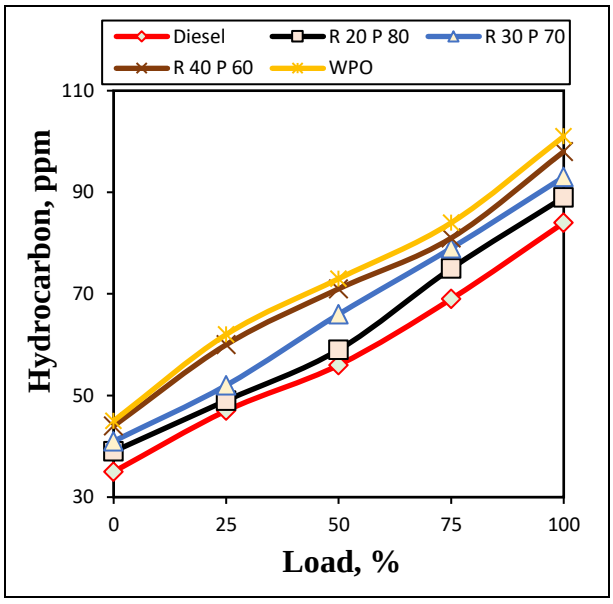


Fig. 13: Variation of HC emission with Load

4.10 Carbon Monoxide Emissions

Carbon monoxide (CO) emissions primarily result from poor air entrainment, insufficient oxygen, a rich mixture, inadequate mixture preparation, and incomplete combustion. CI engines typically operate with excess air, leading to significantly lower CO

emissions compared to spark ignition engines. Nevertheless, these emissions are highly toxic and require strict control. CO is an intermediary combustion product of petroleum fuel, and its emissions depend mainly on the equivalence ratio and the completeness of combustion. However, when complete combustion occurs and the combustion temperature increases, carbon monoxide will be oxidized into carbon dioxide. Fig. 14 illustrates the deviation of CO as load changes. The carbon monoxide emission variations range from 0.1% volume at zero load to 0.65% volume at 100% load for waste plastic oil. For diesel, CO emissions differ from 0.075% volume at zero load to 0.5% volume at full load. Similarly, for the R 40 P 60 blend, CO emissions differ from 0.085% volume at zero load to 0.6% volume at 100% load. CO emissions for the R 30 P 70 mixture span from 0.081% volume under zero load to 0.58% volume under full load, and for the R 20 P 80 blend, they fluctuate between 0.078% volume at zero load and 0.57% volume at 100% load. Fig. 14 demonstrates that CO releases rise with an upsurge in the concentration of rubber seed oil in the mixture. Additionally, the carbon monoxide emissions for WPO and its RSO mixtures are higher than diesel. It is mainly because of the higher viscosity of RSO, resulting in larger fuel spray droplet sizes, local rich regions, and poor mixture preparation.

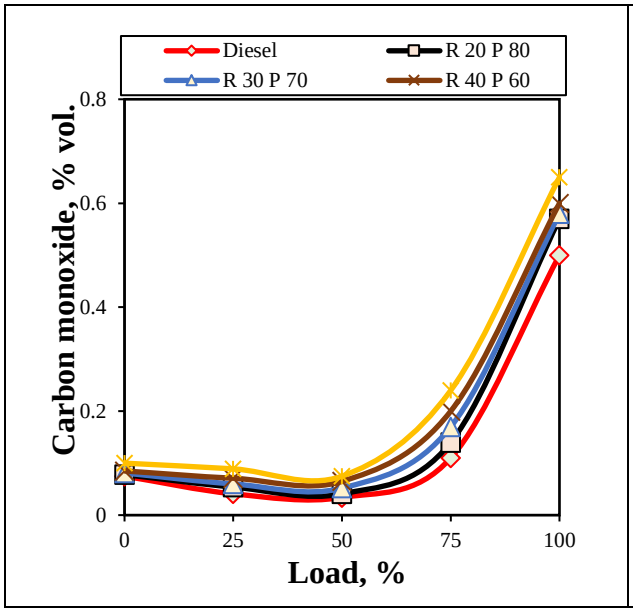


Fig. 14: Variation of CO emission with Load

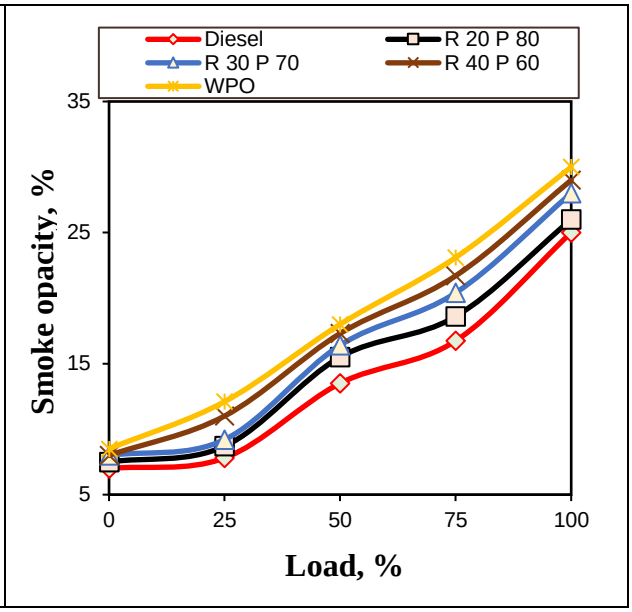


Fig. 15: Variation of Smoke opacity with Load

Table 3. Percentage change of WPO and its RSO blends in comparison with diesel at full load

S. No.	Parameter	R 20 P 80	R 30 P 70	R 40 P 60	WPO
	Combustion parameters				
1	Ignition delay (°CA)	+7.41	+4.63	+1.85	+9.23
2	Maximum heat release (J/°CA)	+9.59	+6.45	+1.37	+13.69
3	Maximum cylinder pressure (bar)	+6.45	+4.84	+1.61	+8.06
	Performance parameters				
1	Brake thermal efficiency (%)	-3.73	-5.97	-7.09	-12.69
2	Brake specific fuel consumption (kg/kWh)	+9.33	+16.8	+20	+24
3	Exhaust gas temperature (°C)	+2.5	+5.5	+8.5	+13.75
	Emission parameters				
1	Oxides of nitrogen emissions (ppm)	+12.19	+6.59	+1.58	+23.17
2	Hydrocarbon emissions (ppm)	+5.95	+10.71	+16.67	+20.24
3	Carbon monoxide emissions (% volume)	+14	+16	+20	+30
4	Smoke opacity emissions (%)	+4	+12	+16	+20
	"+" indicates percentage increase; "-" indicates percentage decrease.				

Table 3 presents the percentage change characteristics of WPO and its RSO blends in comparison to diesel under full-load conditions.

4.11 Smoke Opacity Emissions

Smoke opacity emission refers to the suspension of solid soot particles in the exhaust gases. Soot particle formation predominantly occurs in the central area of each rich fuel droplet under high pressures and temperatures. Smoke opacity emissions are generally higher when the H/C ratio is less than 2. Fig. 15 provides a comparison of smoke opacity emissions for WPO, its RSO mixtures, and diesel under dissimilar loads. It is evident that the opacity emission rises with higher blends and loads. For waste plastic oil, smoke opacity emissions range from 9% under zero load to 30% under full load, while for the R 40 P 60 blend, they vary from 8% under zero load to 29% under 100% load; similarly, for the R 30 P 70 blend, it fluctuates from 8% at zero load to 28% at 100% load, and for the R 20 P 80 blend, it changes from 7.5% at zero load to 26% at 100% load. In diesel, smoke opacity emissions vary from 7% at zero load to 25% at full load. The smoke opacity emissions are slightly higher for WPO and its rubber seed oil mixtures compared to diesel fuel. This increase can be attributed to their greater viscosity, leading to superior mean fuel spray sizes, a reduced air-fuel blending rate, and a higher diffusive combustion phase.

5. CONCLUSION

An investigation was carried out with a single-cylinder, water-cooled CI engine using hybrid alternative biodiesel blends. The performance and emissions of the biodiesel blends were compared to pure diesel and neat waste plastic oil, which yielded the following conclusions:

- The results show that the CI engine can operate with a maximum R 40 P 60 hybrid alternative biodiesel blend; moreover, it was found that R 20 P 80, R 30 P 70, and R 40 P 60 hybrid alternative biodiesel blends lead to poor combustion because of the higher viscosity of RSO. However, it was observed that hybrid alternative biodiesel blends can exhibit a slight increase in peak pressure in comparison to diesel, attributed to their delayed combustion characteristics. But these hybrid alternative biodiesel blends produce a lower peak pressure than neat waste plastic oil. Due to the aforementioned outcomes, these blends experience a maximum heat release rate than diesel.

- The BTHEs of both the neat waste plastic oil and the R 40 P 60 blend are lower in comparison to the other tested fuels. Nevertheless, the R 20 P 80 blend demonstrates the least value of BSFC when contrasted with the R 30 P 70 and R 40 P 60 blends. Also, the EGT is elevated for the R 20 P 80 blend compared to diesel.

- The R 20 P 80 blend exhibits approximately 100 ppm higher NO_x emissions and a 0.07% volume increase in CO emissions when compared to diesel. Furthermore, it demonstrates roughly 5 ppm higher hydrocarbon emissions, along with a 1% rise in smoke opacity emissions compared to diesel. Taking into consideration the combustion, performance, and emission traits, the R 20 P 80 blend emerges as the preferred choice among the three blends.

- The above-mentioned discoveries accentuate the varied potential benefits and applications of hybrid fuel in various fields, including transport, energy generation, agriculture and farming, industrial and commercial uses, and marine and shipping.

List of Symbols and Abbreviations

R 20 P 80	-	20% RSO blended with 80% WPO
R 30 P 70	-	30% RSO blended with 70% WPO
R 40 P 60	-	40% RSO blended with 60% WPO
A/F	-	Air Fuel ratio
ARAI	-	Automotive Research Association of India
BSO	-	Babassu oil
bTDC	-	Before Top Dead Centre, °CA
BP	-	Brake Power, kW
BSFC	-	Brake Specific Fuel Consumption, kg/kWh
BTHE	-	Brake Thermal Efficiency, %
CO	-	Carbon monoxide, % volume
cSt	-	Centi Stoke

DAS	-	Data Acquisition System
EGT	-	Exhaust Gas Temperature, °C
HC	-	Hydro Carbon, ppm
JME	-	Methyl Ester of Jatropha curcas
KME	-	Methyl Ester of Karanja oil
MSW	-	Municipal Solid Waste
NO	-	Nitric Oxide
NO_2	-	Nitrogen Dioxide
NO_x	-	Oxides of nitrogen, ppm
KOH	-	Potassium Hydroxide
SFC	-	Specific Fuel Consumption, kg/kWh
H_2SO_4	-	Sulphuric Acid
VCR	-	Variable Compression Ratio
WPO	-	Waste Plastic Oil
wt.	-	Weight, kg

ACKNOWLEDGMENTS

The authors acknowledge the testing facilities created and provided by the Government College of Engineering, Bargur, India, under TEQIP II funding by MHRD.

DECLARATION OF CONFLICTING INTEREST

The authors declare that they have no known competing financial interests or personal relationships that could have appeared to influence the work reported in this paper.

FUNDING STATEMENT

This research received no specific grant from any funding agency in the public, commercial, or not-for-profit sectors.

DATA AVAILABILITY

The data supporting this study's findings are presented in the article. Additional data can be requested from the corresponding author.

COPYRIGHT

This article is an open-access article distributed under the terms and conditions of the Creative Commons Attribution (CC BY) license (http://creativecommons.org/licenses/by/4.0/).

REFERENCES

Ambarish, D., Samiddha, P. and Bijan, K. M., An experimental study on the performance and emission characteristics of a CI engine fuelled with Jatropha biodiesel and its blends with diesel, *J. Mech. Sci. Technol.,* 28(5), 1961-1966(2014). https://doi.org/10.1007/s12206-014-0344-7

Ananthakumar, S., Jayabal, S. and Thirumal, P., Investigation on performance, emission and combustion characteristics of variable compression engine fuelled with diesel, waste plastics oil blends, *J. Braz. Soc. Mech. Sci. Eng.,* 39(1), 19–28(2017). https://doi.org/10.1007/s40430-016-0518-6

Atul, D. and Avinash, K. A., Performance, emissions and combustion characteristics of Karanja biodiesel in a transportation engine, *Fuel,* 119, 70-80(2014). https://doi.org/10.1016/j.fuel.2013.11.002

Banapurmath, N. R., Tewari, P. G. and Hosmath, R. S., Performance and emission characteristics of a DI compression ignition engine operated on Honge, Jatropha and sesame oil methyl esters, *Renew. Energy,* 33(9), 1982-1988(2008). https://doi.org/10.1016/j.renene.2007.11.012

Buyukkaya, E., Effects of biodiesel on a DI diesel engine performance, emission and combustion characteristics, *Fuel,* 89, 3099-3105(2010). https://doi.org/10.1016/j.fuel.2010.05.034

Chakrabarti, M. H., Mehmood, A., Jafar, N. U., Saeid, B. and Muhammad, S., Technical evaluation of Pongame and Jatropha B20 fuels in Pakistan, *Arab. J. Sci. Eng.*, 38, 759-766(2013). https://doi.org/10.1007/s13369-012-0368-1

Chauhan, B. S., Naveen, K. and Haeng, M. C., A study on the performance and emission of a diesel engine fueled with Jatropha biodiesel oil and its blends, *Energy,* 37(1), 616-622(2012). https://doi.org/10.1016/j.energy.2011.10.043

Gumus, M. and Kasifoglu, S., Performance and emission evaluation of a compression ignition engine using a biodiesel (apricot seed kernel oil methyl ester) and its blends with diesel fuel, *Biomass Bioenergy*, 34(1), 134-139(2010). https://doi.org/10.1016/j.biombioe.2009.10.010

Ikwuagwu, O. E., Ononogbu, I. C. and Njoku, O. U., Production of biodiesel using rubber [Hevea brasiliensis (Kunth. Muell.)] seed oil, *Ind. Crops Prod.,* 12(1), 57-62(2000). https://doi.org/10.1016/S0926-6690(99)00068-0

Ioannis, K., Guohong, T. and Sai, G., Experimental evaluation of a diesel engine fuelled by pyrolysis oils produced from low-density polyethylene and ethylene–vinyl acetate plastics, *Fuel Process Technol.,* 161, 125-131(2017). https://doi.org/10.1016/j.fuproc.2017.03.014

Kumar, S., Prakash, R., Murugan, S. and Singh, R. K., Performance and emission analysis of blends of waste plastic oil obtained by catalytic pyrolysis of waste HDPE with diesel in a CI engine, *Energy Convers. Manage.*, 74, 323-331(2013). https://doi.org/10.1016/j.enconman.2013.05.028

Mani, M., Subash, C. and Nagarajan, G., Performance, emission and combustion characteristics of a DI diesel engine using waste plastic oil, *Appl. Therm. Eng.,* 29(13), 2738-2744(2009). https://doi.org/10.1016/j.applthermaleng.2009.01.007

Miandad, R., Barakat, M. A., Asad, S. A., Rehan, M., Ismail, I. M. I. and Nizami, A. S., Effect of plastic waste types on pyrolysis liquid oil, *Int. Biodeterior Biodegr.*, 119, 239-252(2017). https://doi.org/10.1016/j.ibiod.2016.09.017

Muralidharan, K., Vasudevan, D. and Sheeba, K. N., Performance, emission and combustion characteristics of biodiesel fuelled variable compression ratio engine, *Energy,* 36(8), 5385-5393 (2011). https://doi.org/10.1016/j.energy.2011.06.050

Nantha, G. K. and Thundil, K. R., Effect of pongamia biodiesel on emission and combustion characteristics of DI compression ignition engine, *Ain Shams Eng. J.*, 6(1), 297-305(2015). https://doi.org/10.1016/j.asej.2014.10.001

Nurun, N. M., Mustafizur, R. M. and Shamim, A. M., Biodiesel from cotton seed oil and its effect on engine performance and exhaust emissions, *Appl. Therm. Eng.*, 29(11-12), 2265-2270(2009). https://doi.org/10.1016/j.applthermaleng.2008.11.009

Ozcanli, M., Serin, H., Saribiyik, O. Y., Aydin, K. and Serin, S., Performance and emission studies of Castor Bean (Ricinus Communis) oil biodiesel and its blends with diesel fuel, *Energy Sources Recovery Util. Environ Eff.*, 34, 1808-1814(2012). https://doi.org/10.1080/15567036.2010.545800

Pritinika, B. and Murugan, S., Combustion, performance and emission parameters of used transformer oil and its diesel blends in a DI diesel engine, *Fuel,* 104, 147-154(2013). https://doi.org/10.1016/j.fuel.2012.09.077

Rakopoulos, C. D., Antonopoulos, K. A., Rakopoulos, D. C., Hountalas, D. T. and Giakoumis, E. G., Comparative performance and emissions study of a direct injection diesel engine using blends of diesel fuel with vegetable oils or bio-diesels of various origins, *Energy Convers. Manag.,* 47(18-19), 3272-3287(2006). https://doi.org/10.1016/j.enconman.2006.01.006

Ramadhas, A. S., Jayaraj, S. and Muraleedharan, C., Biodiesel production from high FFA rubber seed oil, *Fuel,* 84(4), 335-340(2005a). https://doi.org/10.1016/j.fuel.2004.09.016

Ramadhas, A. S., Muraleedharan, C. and Jayaraj, S., Performance and emission evaluation of a diesel engine fueled with methyl esters of rubber seed oil, *Renew. Energ.*, 30(12), 1789-1800(2005b). https://doi.org/10.1016/j.renene.2005.01.009

Reshad, A. S., Prasenjit, B., Ashish, J., Chaudhari, P. T., Vinayak, K., Vaibhav, V. G. and Niranjan, S., Rubber seed oil methyl ester (ROME) synthesis, engine performance and emission characteristics of blends, *Energy Fuels*, 29(8), 5136–5144(2015). https://doi.org/10.1021/acs.energyfuels.5b01033

Sahoo, P. K. and Das, L. M., Combustion analysis of Jatropha, Karanja and Polanga based biodiesel as fuel in a diesel engine, *Fuel,* 88(6), 994-999(2009a). https://doi.org/10.1016/j.fuel.2008.11.012

Sahoo, P. K., Das, L. M., Babu, M. K. G., Arora, P., Singh, V. P., Kumar, N. R. and Varyani, T. S., Comparative evaluation of performance and emission characteristics of Jatropha, Karanja and Polanga based biodiesel as fuel in a tractor engine, *Fuel,* 88(9), 1698-1707(2009b). https://doi.org/10.1016/j.fuel.2009.02.015

Saravanan, S., Nagarajan, G. and Lakshmi, N. R. G., Feasibility analysis of crude rice bran oil methyl ester blend as a stationary and automotive diesel engine fuel, *Energy Sustain. Dev.*, 13(1), 52-55(2009). https://doi.org/10.1016/j.esd.2009.03.001

Senthilkumar, P. and Sankaranarayanan, G., Effect of Jatropha methyl ester on waste plastic oil fueled DI diesel engine, *J. Energy Inst.*, 89(4), 504-512(2016). https://doi.org/10.1016/j.joei.2015.07.006

Subbarayan, M. R. and Senthil, K. J. S., A study of performance and emissions of direct injection diesel engine fuelled with cotton seed oil methyl ester and pumpkin seed oil methyl ester and its blends with diesel using exhaust gas recirculation, *Biofuels,* 6(3-4), 171-177(2015). https://doi.org/10.1080/17597269.2015.1065599

Sureshkumar, K., Velraj, R. and Ganesan, R., Performance and exhaust emission characteristics of a CI engine fueled with *Pongamia pinnata* methyl ester (PPME) and its blends with diesel, *Renew. Energy*, 33, 2294-2302(2008). https://doi.org/10.1016/j.renene.2008.01.011

Vijayaraj, K. and Sathiyagnanam, A. P., Experimental investigation of a diesel engine with methyl ester of mango seed oil and diesel blends, *Alex. Eng. J.*, 55(1), 215-221(2015). https://doi.org/10.1016/j.aej.2015.12.001